Archives of Hydro-Engineering and Environmental Mechanics
Vol. 48 (2001), No. 2, pp. 17–29

Marine Parameters from Radar Satellite Data

S. Lehner,* J. Schulz-Stellenfleth,* J. Horstmann**

* German Aerospace Center (DLR), Institute of Remote Sensing Technology,
PF 1116 D-82230 Weßling, Germany
e-mail: Susanne.Lehner@dlr.de
** GKSS Research Center, Max Planck Str., 21502 Geesthacht

Abstract

In 2001 the European Space Agency ESA will launch the earth observation satellite ENVISAT. It will carry several instruments that provide new opportunities to measure oceanographic variables. These are the Advanced Synthetic Aperture Radar (ASAR), the Radar Altimeter (RA), the Medium Resolution Imaging Spectrometer (MERIS) and the Advanced Along-Track Scanning Radiometer (AATSR). Together, they represent the main measurement techniques of satellite oceanography, and complement each other perfectly. These instruments are to be used in synergy to:

- improve the analysis of measured wind and ocean wave fields, and thereby improve weather forecasting at weather centers;
- determine the extent and variables of sea ice and develop a five-day sea ice prediction model, to support maritime shipping and offshore activities;
- monitor map sediment and suspended matter transport in coastal regions, especially in areas with large river estuaries, which greatly affects shipping lanes, harbours, and dredging activities;
- monitor hydrobiological and bio-geochemical variables related to water quality in coastal regions and large inland waters, which affects ecology, coastal development, aquaculture, drinking water supplies, and tourism.

To prepare the oceanographic community to make best use of the ENVISAT sensors in the pre-launch phase, existing algorithms to derive marine parameters are used and validated using data from the ERS SAR, the ERS RA, SeaWiFS, and IRS MOS sensors now in operation. Derived products, which include wind field, sea state, sea level, sea surface temperature and concentrations of water constituents, are used to address problems that can be tackled best using the synergy of radar and optical data, such as the effect of surface slicks on radar wind measurements, sea state on ocean color, wind and waves on the resuspension of suspended matter, and wind and waves on sea ice variables.

1. Introduction

Satellites launched in the last two decades provide a completely new global view of the earth. The use of this information is a prerequisite for the sustainable utilization and management of our environment. For example weather and climate parameters are acquired from surface measurements by remote sensing satellites.

One of the grand challenges in marine research is the design and implementation of an operational monitoring system which comprises observation of physical and bio-geochemical variables and the integration of data into operational forecasting models and oceanographic information systems. The establishment of information systems and prediction models is the basis for managing the use of natural resources such as marine life and minerals, for managing traffic, coastal protection, the preservation of biodiversity, and natural habitats, recreation and tourism and the increasing pressure of urbanization on coastal zones. Complementary to oceanographic monitoring programs, inland waters also require similar ongoing observations for their sustainable use and development as reservoirs for clean drinking water, transportation passageways, natural habitats, and recreational areas.

Satellite remote sensing as an important element of operational observation systems provides rapid global and regional views of key variables such as surface wind and waves, sea surface temperature, ice, currents, distribution of water constituents, optical properties of the sea, characteristics of shorelines and coastal zone habitats, and land use. Until now research was mainly concentrated on the development of methods for single sensors. With the launching of a new generation of earth observation satellites the synergistic use of multiple sensors and integration of remote sensing into operational observation systems will come into focus. One satellite of particular interest for comprehensive observations of sea and inland waters is ENVISAT operated by the European Space Agency ESA. With its launching in mid-2001 it will be the first satellite to integrate instruments for simultaneous observations of physical and bio-geochemical variables. Although ENVISAT is a research satellite, it will allow the integration of remote sensing data into operational observation systems.

The following ENVISAT sensors and observation techniques will be of interest for oceanographic applications (cf. Figure 1):

1. The Advanced Synthetic Aperture Radar (ASAR) and the Radar-Altimeter (RA-2) for the determination of wind, waves, and sea ice.
2. The Medium Resolution Imaging Spectrometer (MERIS) for the determination of phytoplankton, suspended matter (SPM), dissolved organic carbon, and the attenuation of photosynthetically available radiation (PAR) in water.
3. The Along Track Scanning Radiometer (ATSR) for the determination of Sea Surface Temperature (SST).

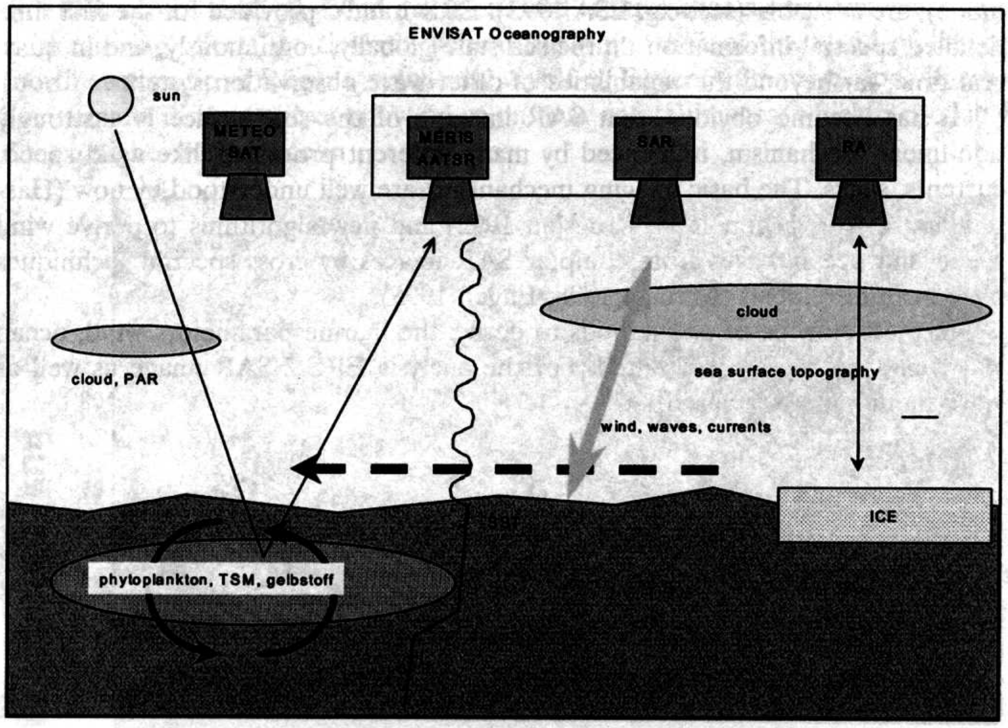

Fig. 1. Satellite sensors and measurable marine parameters

At present similar sensors, which can be used for the improvement and development of algorithms and validation of data products are in orbit:

- radar sensors on the European Remote Sensing satellites (ERS-1/2) and Canadian satellite RADARSAT;
- optical sensors on NOAA, MODIS, MOS (on IRS-P3).

This article presents a overview of the synergetic use of satellite data to extract marine parameters from satellite data and synergy effects. In the first section some algorithms to extract parameters like surface wind and waves from radar data are presented. The second section gives some examples for combining the information from different sensors and the study of synergy effects. The last section contains a short summary and concluding remarks.

2. Marine Parameters from SAR Data

Since 1991 Synthetic Aperture Radars (SAR) (see, e.g. Bamler and Schättler 1993) on ERS satellites have been imaging the ocean surface. Full swath images of 100 × 100 km near the coast (so-called image mode), as well as global data sets of small imagettes of 5 × 10 km in size every 200 km along the orbit (so-called wave mode), are available (see, e.g. ESA 1993). ERS-1 and 2 provided for the first time detailed spectral information on the sea state globally, continuously, and in quasi real time, far beyond the capabilities of other wave observation systems.

It has become obvious, that SAR imaging of the sea surface is a strongly non-linear mechanism, influenced by many different processes, like wind speed, currents, slicks. The basic imaging mechanisms are well understood by now (Hasselmann 1991, Vachon 1994, Krogstad 1992) and new algorithms to derive wind speed and ocean waves from complex SAR images by cross spectral techniques have been developed (Kerbaol 1998, Engen 1995).

In the following some methods to derive the marine parameters wind, ocean waves and sea ice are presented. For the analysis ERS-2 SAR image as well as wave mode data were used.

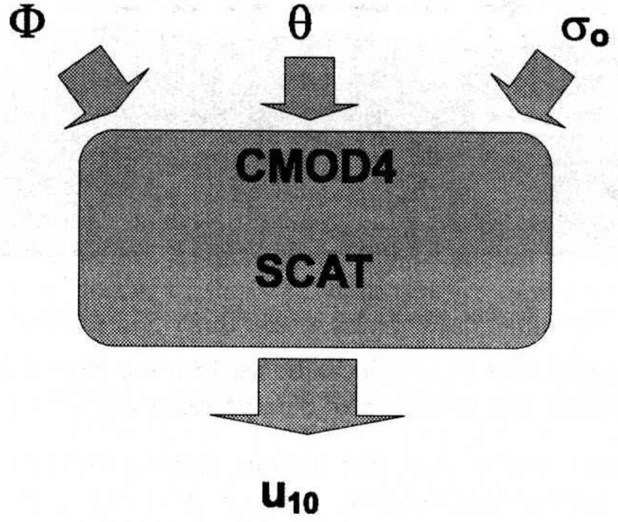

Fig. 2. Scheme to derive wind speed u_{10} from angle Φ between wind direction and antenna, incidence angle Θ and calibrated radar backscatter σ_0 using the scatterometer algorithm CMOD4

2.1. Wind Fields from SAR

CMOD4 is an algorithm that was originally developed to determine wind speed from the ERS scatterometer (SCAT). As the SCAT and the SAR both operate on C-band it can be used on SAR data as well. The method is based on converting grey levels of SAR images into normalized calibrated radar cross-section (NCRS) using the ESA calibration algorithm (Laur 1996). Wind speed is derived using the semi empirical CMOD4 algorithm (Stoffelen and Anderson 1993) and some additional information on wind direction. Usually, SAR images show distinct features like wind induced streaks or shadowing behind coasts from which the wind direction can be derived. Wind directions and relative changes in wind speed due to shadowing effects, particularly behind the white cliffs of the island of Rügen (north eastern tip of Rügen), are clearly visible in Figure 3. On wave mode images not as many distinct stripes show up as on near coastal images, which is probably due to higher turbulence in coastal areas.

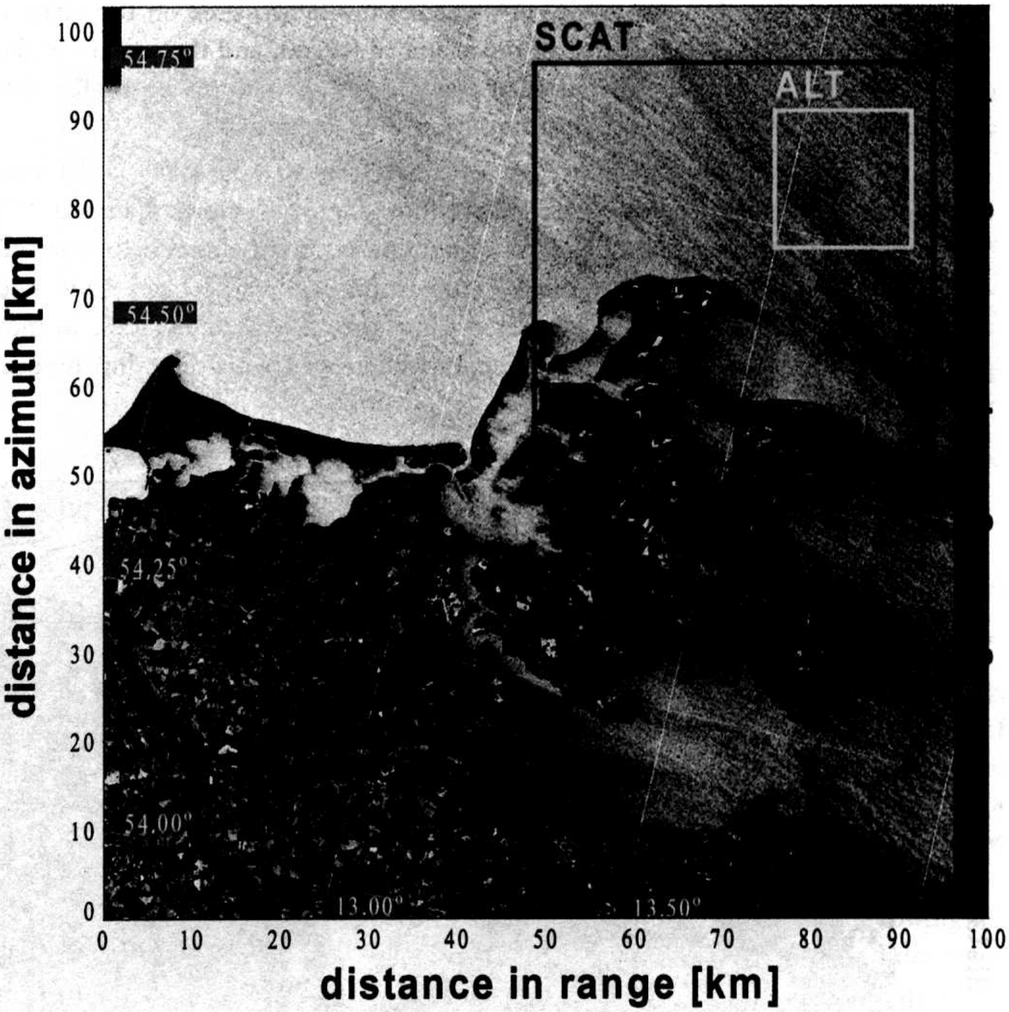

Fig. 3. ERS SAR image of the island of Rügen in the Baltic Sea showing wind streaks and wind shadowing behind the cliffs. For comparison the resolution cells of scatterometer and altimeter are given

The overall close conformity of ERS SAR derived wind fields with in situ measurements constitutes motivation for comparing SAR retrieved wind speeds over the entire image. Furthermore, it is important to test the capability of the algorithms to reproduce the spatial variation of wind fields. Since no measuring method exists covering the entire region similar to an ERS SAR image with high spatial resolution, the mesoscale atmospheric model, Geesthacht simulation model of the atmosphere (GESIMA), was used to compute the wind field for comparison. GESIMA is a 3 dimensional non-hydrostatic model of the atmospheric circulation with terrain-following coordinates. A detailed description of the model is given by Kapitza and Eppel (1992). GESIMA was set up at two sites on the coast of the Baltic Sea. The first is the area of the island of Rügen, and the second in that of the Odra lagoon and the Pomeranian Bay. These areas were chosen for their complex structure of wind field, resulting from the topography.

To retrieve the wind direction each ERS SAR image was analysed for wind induced streaks using the FFT-based algorithm. Figure 4 shows a cutout of a SAR image of the Odra lagoon. The superimposed wind directions represent wind directions as computed by the FFT algorithm where the black solid lines represent the wind direction as computed for 5 km × 5 km subimages. In most parts of the image, retrieved wind directions align well with the wind induced streaks visible in the SAR image.

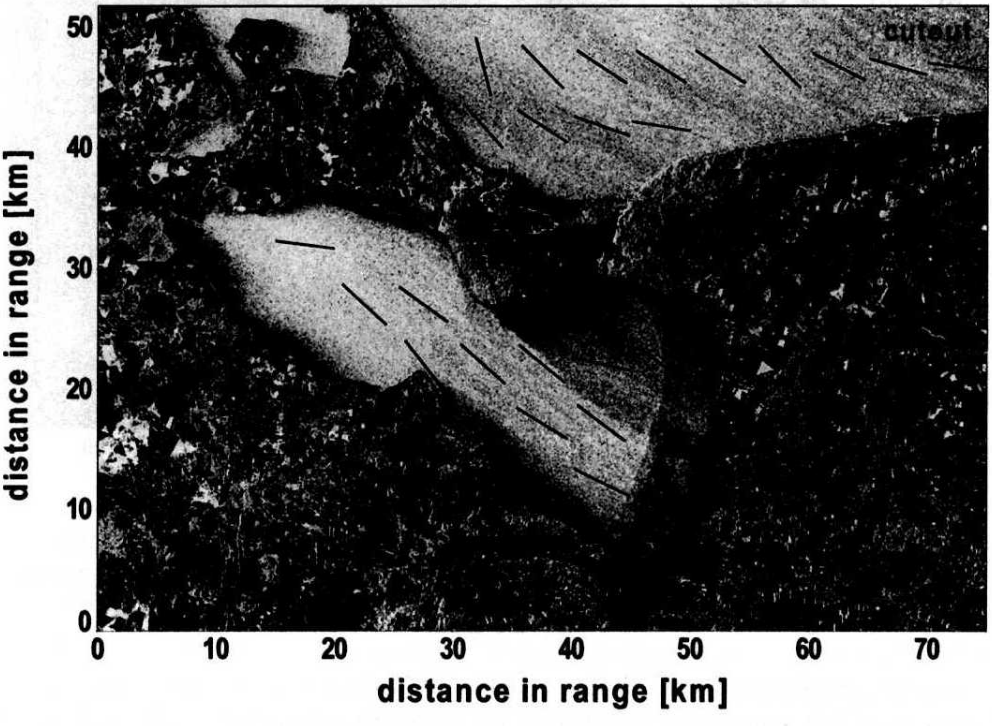

Fig. 4. ERS SAR image of the Odra lagoon and the Baltic Sea showing wind direction derived from wind streaks

In both cases the 180° directional ambiguity can be removed due to the wind shadowing of the land which is particularly visible on the lee side of the coast. The mean wind direction resulting from the SAR images around Rügen was 290° and in the Odra estuary 300°. These wind directions were taken as input to the C-band models to obtain the wind speed over the water surface. In Fig. 5 left hand side the resulting isotaches are given for the Odra lagoon.

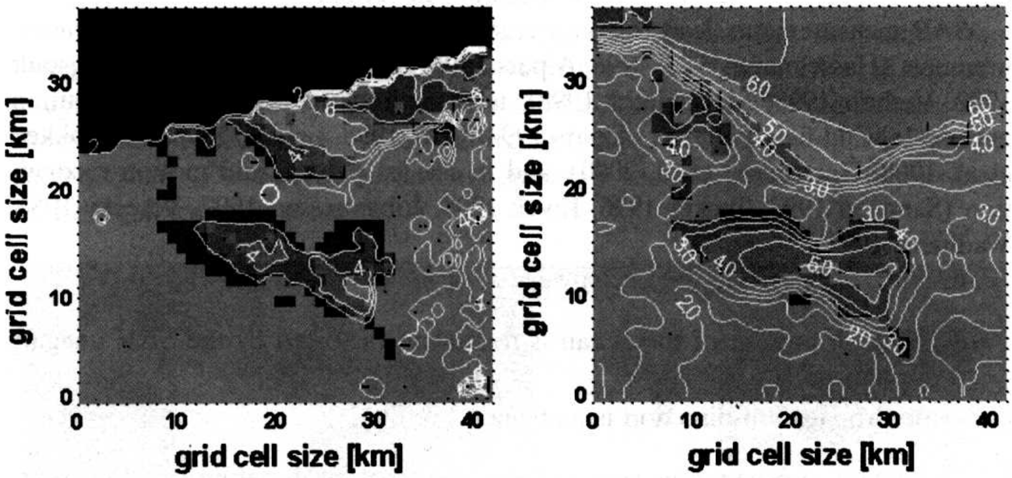

Fig. 5. SAR derived wind speed (left) from the image shown in Figure 4 in comparison with wind speed calculated using the GESIMA mesoscale wind speed model

For this comparison, GESIMA was run assuming neutral stability, with 8 layers between 0 m and 1500 m in the vertical and a fixed horizontal grid cell size of 2 km in the region of the Odra estuary. The lower boundary condition for the friction velocity over the sea was given by Charnock's relation while over land a variable bottom stress was taken into account according to land use maps. The results of the GESIMA model are plotted on the right hand side of Fig. 5.

The magnitude of wind speeds agrees overall quite well. Wind shadowing effects show the same order of magnitude. However, comparisons show differences in the geographical location of the wind shadowing effects and a much smoother solution from GESIMA. GESIMA seems to overestimate the effect of wind shadowing, which could be due to uncertainties in the land use maps. Furthermore, throughout the considered areas SAR retrieved wind fields show much finer detail of the wind structure and a much higher variability of the wind. This is due to the difference between the snapshot of the SAR image, giving an instantaneous appearance of a highly turbulent wind field, the mesoscale model simulation assuming a stationary situation. It is shown that the wind retrieval algorithms allow the extraction of wind fields to resolve spatial inhomogenities in the wind field, which in these cases are mainly due to the variable topography and the variable bottom stress of the atmosphere over land.

2.2. Ocean Waves

Spaceborne SAR is so far the only instrument providing global information on the 2 dimensional ocean wave spectrum on a continuous basis, including information on wave height, wave length, and propagation direction.

SAR measurements lead to considerable improvements in ocean wave measurements (Hasselmann 1985, 1996, Alpers 1996, Bao 1997, Bauer 1998, Krogstadt 1992, Vachon 1998, Melsheimer 1998), new methods to obtain high resolution mesoscale wind field patterns (Alpers 1994, 1996, 1998, Lehner 1998, Korsbakken et al. 1998, Horstmann et al. 2000), and in sea ice pattern and motion recognition (Sandven 1993, Tucker 1996, Kwok 1998, Johannessen 1997, Vesecky 1988, Wadhams 1991).

Problems in deriving the ocean wave spectra are:

- the wave pattern of the ocean is nonlinear, distorted by the SAR imaging mechanism.
- the propagation direction is ambiguous.

Derivation of ocean wave spectra from cross spectra therefore requires inversion techniques using some kind of a priori knowledge (Hasselmann 1991, Engen 1995).

Apart from the 100 × 100 km images as shown in Ffigure 3 a dataset consisting of radar images 5 × 10 km in size, available every 200km along the satellite track was acquired on a global and continuous basis. These so-called imagettes were further processed by ESA to so-called UWA spectra, data sets from which ocean wave spectra can be calculated using SAR inversion methods (Heimbach 1998), which is state-of-the art at the European Center of Medium Range Weather Forecasts (ECMWF).

New processing methods resulting in complex imagettes give the opportunity to derive two appearances separated in time by approximately half a second. Using these multilook techniques, newly developed algorithms (Engen 1995, Bao and Alpers 1996, Lehner 1998) are used to infer the propagation direction of the waves and to derive ocean wave spectra.

Although even swell systems with high phase speeds only move a fraction of one image pixel in this time period, the phase shift can be detected in the cross spectrum. Compared to the classical image spectrum, the cross spectrum has been shown to have two major advantages:

- it provides an estimate of the image spectrum that is not biased by pedestal noise.

- it contains information on the wave propagation direction and phase speed.

Complex imagettes will be available from ENVISAT's ASAR and their operational use is planned at meteorological centres. Using the imagettes instead of spectra additionally yields the opportunity to study ocean surface features, such as the statistical distribution of natural slicks. In the study of Lehner et al. (2000) a first assessment of the statistical properties of a global set of cross spectra is presented.

Figure 6 shows global sea state measurements for one day. Each arrow represents a measurement of significant wave height derived from a 5 × 10 km radar image, as acquired every 200 km along the satellite track. The red crosses mark the available NOAA buoys. The small radar image at the upper right is from the Indian Ocean. The derived ocean wave spectrum shows a 600 m long swell system of 4 m significant wave height.

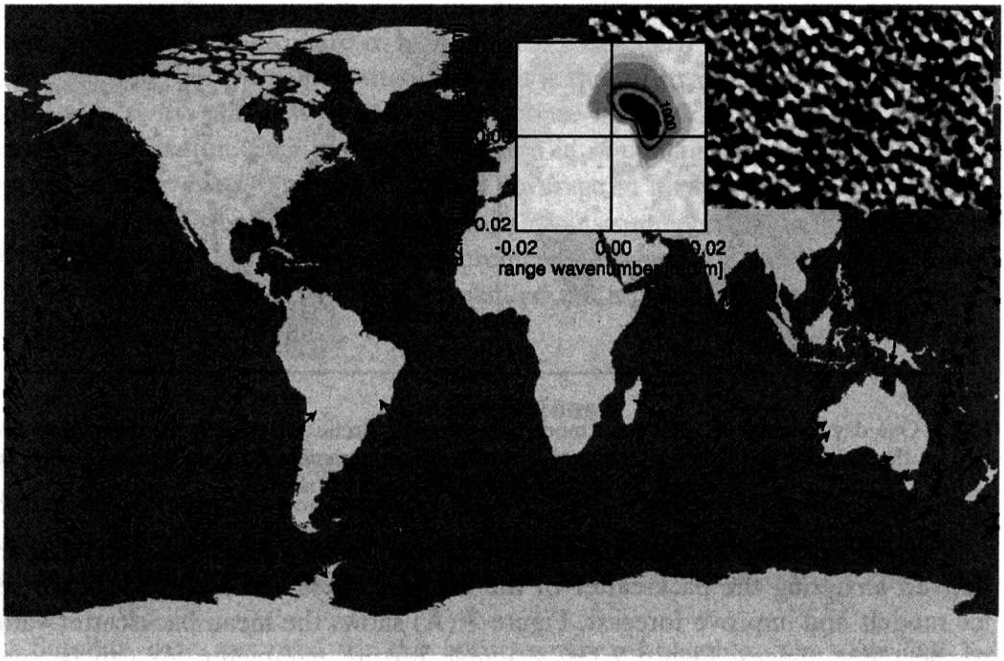

Fig. 6. SAR wave mode data. A SAR 5 × 10 km imagette is shown together with the ocean wave spectrum derived by inversion methods. The distribuition of derived wave propagation is shown on the map in the background

2.3. Sea Ice

Maps of sea ice are essential for ship routing, but also important for glaciological and climatological studies. The extension of ice coverage as well as properties of the ice such as thickness and roughness are of interest. The goal is to combine data of RA (information about ice thickness, but low resolution only along a track) and ASAR (high horizontal resolution, but no information about thickness) to derive this information and provide near real time ice maps.

Several studies were undertaken to determine sea ice variables such as extension, roughness and thickness from SAR images (Kwok et al. 1998, Gohin et al. 1998, Korsnes 1998, Johannessen et al. 1997, Sandven et al. 1997). Global studies using SAR data have not been undertaken up to now. In particular, globally available wave mode data has not been exploited yet. Figure 7 shows the synoptic coverage of the arctic area by imagettes acquired over the period of one day (June, 1, 1997), here the coverage is especially dense.

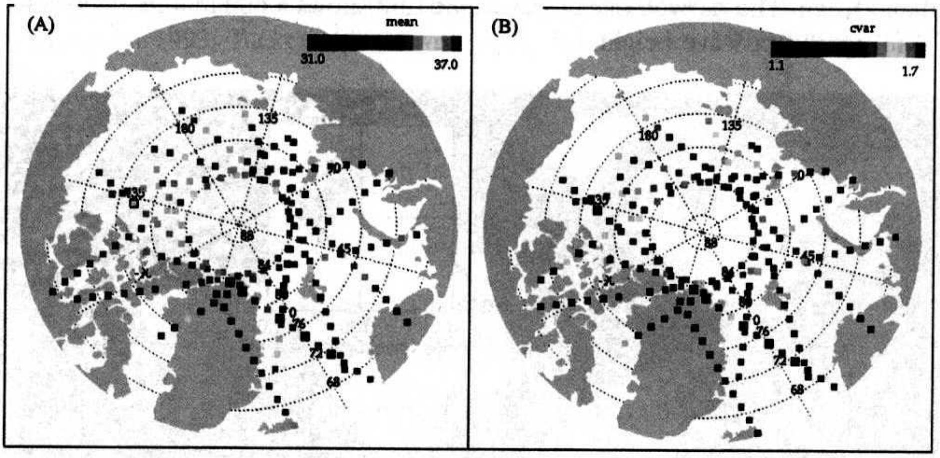

Fig. 7. One day coverage of SAR wave mode data over the Arctic. On the left the mean grey level and on the right the coefficient of variance is shown. These parameters are used to determine sea ice type to validate and improve sea ice models

Sea ice variables like deformation energy or pressure ridge concentration are derived analyzing the backscatter of the images. These are used to validate sea ice models and improve forecast. Figure 7 (A) shows the mean backscatter value of the radar images, Figure 7 (B) a simple texture parameter. As can be seen on these figures, land ice and open water have low texture with high backscatter values (bright). The backscatter and texture of sea ice depends on ice parameters, so backscatter analyzing can be used to extract ice parameters.

3. Synergy with Optical Data

Global satellite optical data were not available until 1986. After the operation of the Coastal Zone Color Scanner (CZCS) was terminated in 1986, the relevant user communities could not be provided with new data until the launch of MOS on PRIRODA and IRS in 1996 (Zimmermann et al. 1993) and of SeaWiFS on SeaStar in 1997. While the use of CZCS data concentrated mainly on medium and large scale features in ocean waters, the new sensors with narrow spectral bands like MOS and MERIS and improved spatial resolution will open new applications in coastal zones (Doerffer et al. 1989) and inland waters (Tilzer and Beese 1991, Prézelin 1991, Haese et al. 1998). ESA's new satellite ENVISAT will carry advanced instruments on board, which, for the first time, will enable the exploiting of the synergy of radar and optical instruments, and, thus, to obtain a new perspective of the ocean.

Methods of using the synergy of the derived hydrophysical and hydrobiological variables can either improve algorithms for one instrument, or derive variables which can only be determined when data of different instruments are combined. Main applications are new models of ocean biomass production, which is a key element in the global carbon cycle and, thus, an essential factor in climate dynamics studies, and the starting point of the marine food web. Time series of detailed maps of SPM distribution are of high interest particularly for coastal waters. SPM is the main carrier of many contaminants, it is the substrate for biological decomposition activity, and controls the light climate in water, which is important for primary production. One particular problem in obtaining dense time series from optical satellite instruments is the cloud coverage in many areas.

Algorithms using the synergy of available instruments will analyze the effect of surface slicks on radar wind measurements, sea state on ocean colour, wind and waves on the resuspension of suspended matter, and wind and waves on sea ice variables.

4. Conclusions

Recent advances in oceanography and sea ice research using observations by the European Remote Sensing satellites ERS-1, ERS-2 cover a wide range of topics including algorithm development, geophysical parameter retrieval and validation studies on near surface winds, surface waves, oceanic features, oceanic circulation and polar sea ice.

Satellite data are used for the improvement of weather, sea state and ice forecasts, for shiprouting, offshore operations and coastal protection. Water quality variables including phyto-plankton and primary production are monitored and time series of these variables are generated to improve the knowledge about ocean variability, coastal morphodynamics, and the transport of suspended matter.

Acknowledgments

We thank R. Doerffer, GKSS for providing Figure 1. The research was funded by BMBF in the framework of the HGF project ENVOC.

References

Alpers W., Brümmer B. (1994), Atmospheric boundary layer rolls observed by the synthetic aperture radar aboard the ERS-1 satellite, *J. Geophys. Res.*, 99, 12613–12621.

Alpers W., Stilke G. (1996), Observations of a nonlinear wave disturbance in the marine atmosphere by the synthetic aperture radar aboard the ERS-1 satellite, *J. Geophys. Res.*, 101, 6513–6525.

Alpers W., Pahl U., Gross G. (1998), Katabatic wind fields in coastal areas studied by ERS-1 Real aperture radar imagery and numerical modeling, *J. Geophys. Res.*, 103, 7875–7886.

Bamler R. (1992), A systematic comparison of SAR focusing algorithm, *IEEE Trans. on Geosci. and Rem. Sens.*, 1005–1009.

Bao M., Brüning C., Alpers W. (1997), Simulation of ocean wave imaging by an along-track interferometric synthetic aperture radar, *IEEE Trans. on Geosci. and Rem. Sens.*, 618–631, 35.

Bauer E., Hasselmann S., Hasselmann K., Graber H. C. (1992), Validation and assimilation of SEASAT altimeter waves heights using the WAM model, *J. Geophys. Res.*, 97, 12671–12682.

Engen G., Johnson H. (1995), SAR-ocean wave inversion using image cross spectra, *IEEE Trans. Geosci. Rem. Sens.*, 33, 1047–1056.

Hasselmann K., Raney R. K., Plant W. J., Alpers W., Shuchman R. A., Lyzenga D. R., Rufenach C. L., Tucker M. J. (1985), Theory of synthetic aperture radar ocean imaging: A MARSEN view, *J. Geophys. Res.*, 90, 4659–4686.

Hasselmann K., Hasselmann S. (1991), On the nonlinear mapping of an ocean wave spectrum into a synthetic aperture radar image spectrum, *J. Geophys. Res.*, 96, 10713–10729.

Hasselmann S., Brüning C., Hasselmann K., Heimbach P. (1996), An improved algorithm for the retrieval of ocean wave spectra from synthetic aperture radar image spectra, *J. Geophys. Res.*, 101, 16615–16629.

Horstmann J., Koch W., Lehner S., Tonboe R. (2000), Wind Retrieval over the Ocean using Synthetic Aperture Radar with C-Band HH-Polarization, *IEEE, TGARSS*, Vol. 38, No. 5, 2122–2131.

Johannessen O. A., Sandven S., Kloster K., Pettersson L. H., Melentyev V. V., Bobylev L. P., Kondratyev K. (1997), ERS-1/2 SAR monitoring of dangerous ice phenomena along the western part of northern sea route, *Int. J. Rem. Sensing*, 18, 2477–2481.

Krogstad H. (1992), A simple derivation of Hasselmann's nonlinear ocean-synthetic aperture radar transform, *J. Geophys. Res.*, 97, 2421–2425.

Lehner S., Dech S. W., Holz A., Meisner R., Niederhuber M., Tungalagsaikhan P. (1997), Operational determination of satellite derived sea surface temperature and wind speed from NOAA AVHRR and ERS SAR images, *Elsevier Oceanography Series*, Vol. 62, 243–250.

Lehner S., Horstmann J., Koch W., Rosenthal W. (1998), Mesoscale wind measurements using recalibrated ERS SAR images, *J. Geophys. Res.*, Vol. 103, 7847–7856.

Lehner S., Schulz-Stellenfleth J., Schättler B., Breit H., Horstmann J. (2000), Wind and Wave measurements using complex ERS-2 wave mode data, *IEEE, TGARSS*, Vol. 38, No. 5, 2246–2257.

Melsheimer Ch., Bao M., Alpers W. (1998), Imaging of ocean waves on both sides of an atmospheric front by the SIR-C/X-SAR multifrequency synthetic aperture radar, *J. Geophys. Res.*, 103, 18839–18849.

Niedermeier A., Romaneeßen E., Lehner S. (2000), Coastlines in SAR Images using Edge detection by Wavelet Methods, *IEEE, TGARSS*, Vol. 38, No. 5, 2270–2281.

Prézelin B. B., Tilzer M. M., Schofield O., Haese C. (1991), The control of the production process of phytoplankton by the physical structure of the aquatic environment with special reference to its optical properties, *Aquatic Sciences* 53, 136–186.

Sandven S., Kloster K., Johannessen O. M., Miles M. (1993), SIZEX 92-ERS-1 SAR ice validation experiment, *NERSC*, No. 69.

Tilzer M. M., Beese B. (1998), The seasonal productivity cycle of phytoplankton and controlling factors in Lake Constance, *Schweiz. Z. Hydrol*, 50(1), 1–39.

Vesecky J. F., Samadani R., Smith M. P., Daida J. M., Bracewell R. N. (1988), Observation of sea-ice dynamics using synthetic aperture radar images: automated analysis, *IEEE Trans. on Geosci. and Rem. Sens.*, Vol. 26, 38–48.

Wadhams P., Holt B. (1991), Waves in frazil and pancake ice and their detection in seasat synthetic aperture radar imagery, *J. Geophys. Res.*, 96, 8835–8852.